21. Corona.

Solar Corona

- Coronal Structure
- Emission Lines
- X-ray Emission
- Scaling Laws
- Heating of Coronal Loops

- On-line book: Markus J. Aschwanden, Physics of the Solar Corona: http://www.lmsal.com/~aschwand/eprints/2004_book/

Temperature structure of the solar atmosphere

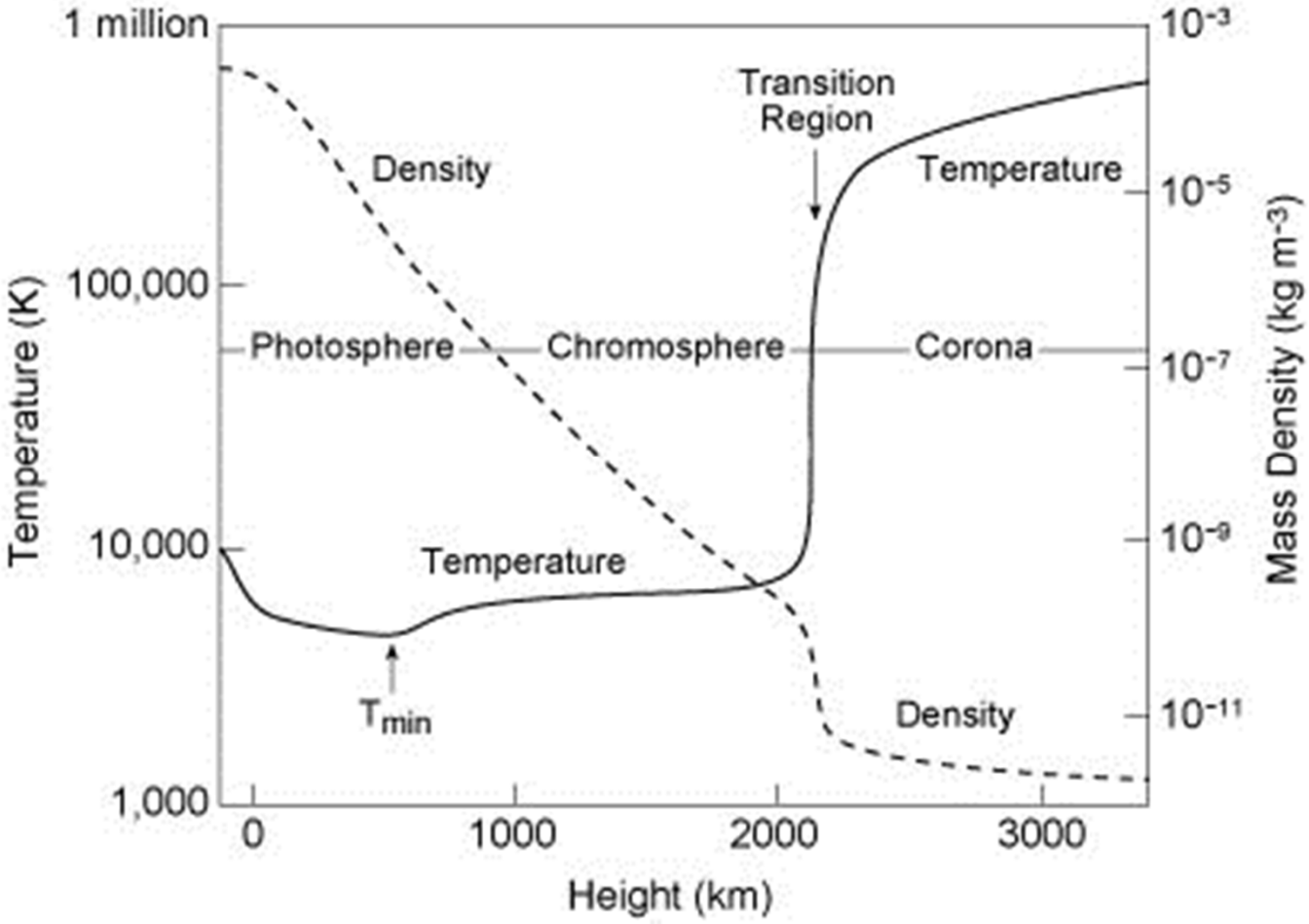

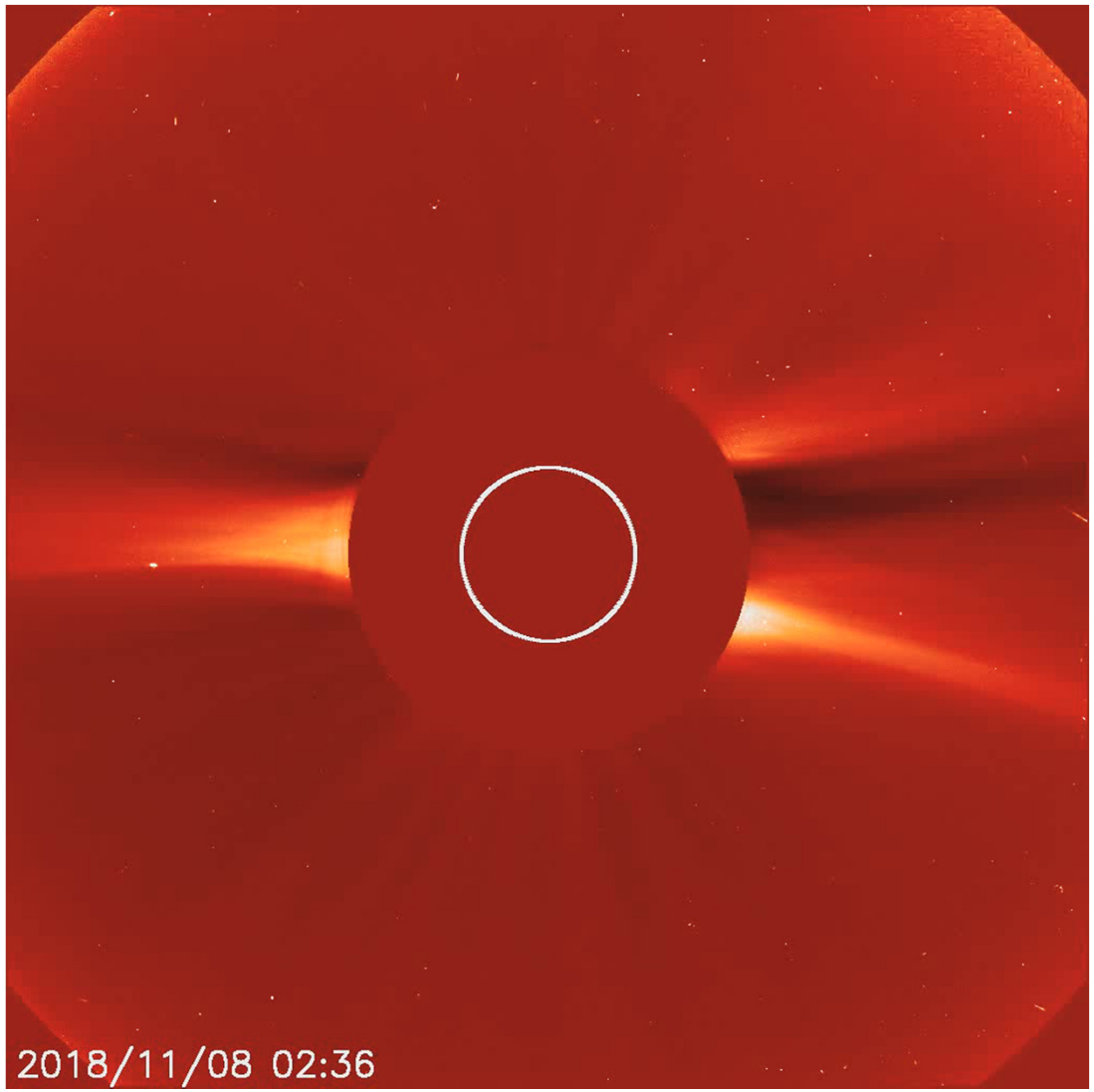
2018/11/08 02:36

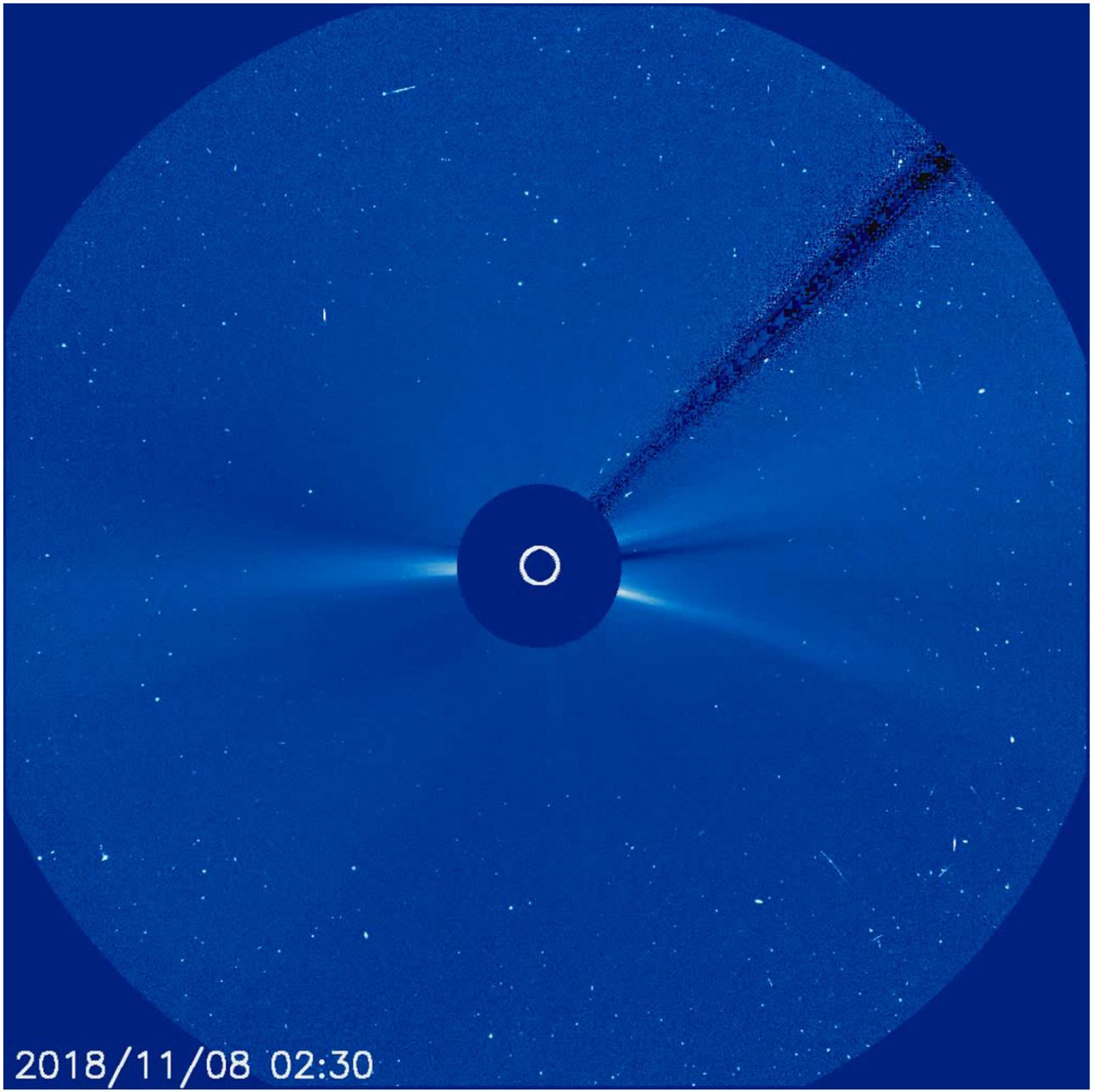
2018/11/08 02:30

About the Solar Corona

The solar corona is composed of gas, dust, molecules, and magnetic fields that constantly stream from the Sun's surface.

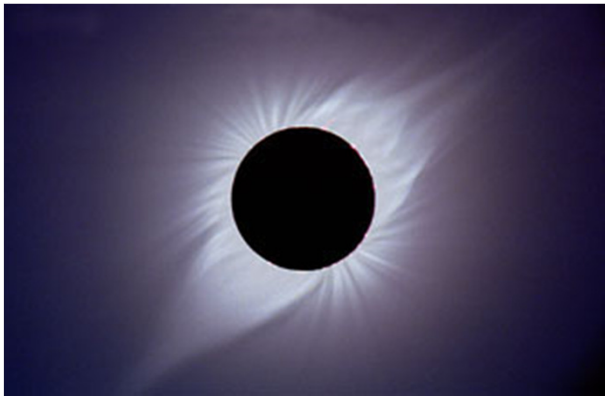

Image Credit Fred Espenak

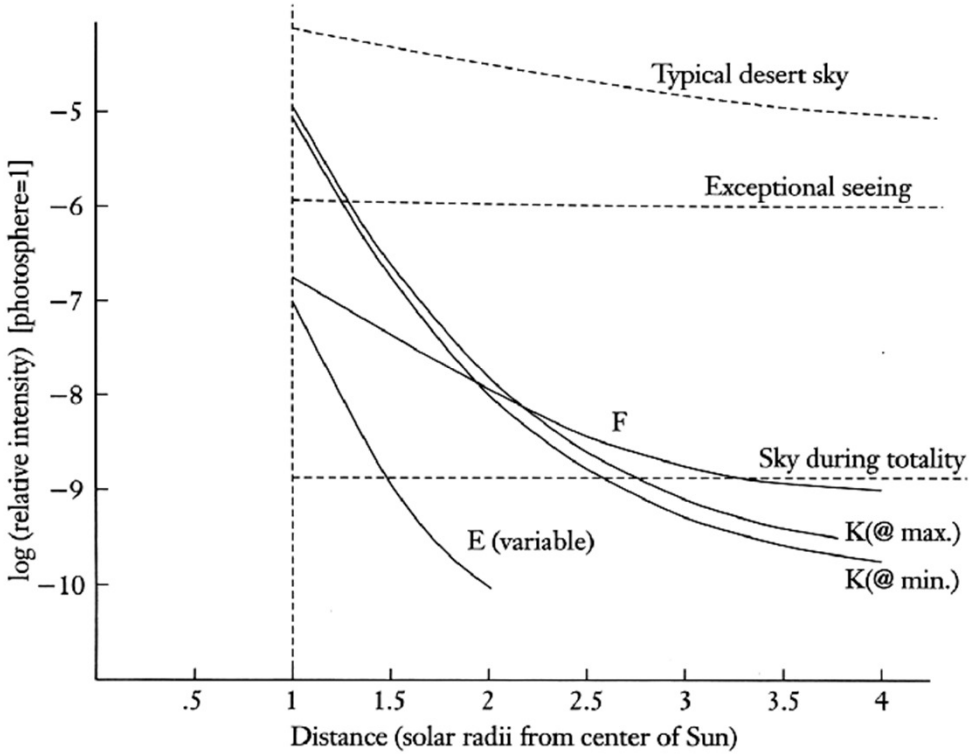

Image credit Golub 2001.

Four Coronal Components:

1. K-corona, scattering on electrons.
2. F-corona, scattering on dust particles.
3. E-corona, emission lines produced by ions in the corona.
4. T-corona, thermal emission of dust particles.

Coronal Structure

The solar corona is diffuse, hot plasma extending a solar radius or more above the surface of the Sun. The corona is only visible in white light during total eclipses, because its intensity is about 10^{-6} of that of the Sun's disk (roughly the brightness of the full moon).

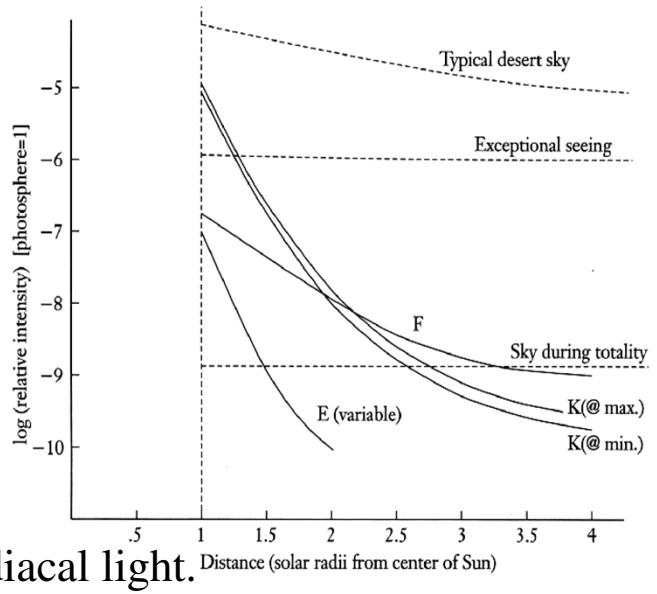

The observed light has several components.

- The **F corona** exhibits the Fraunhofer lines, because it is photospheric light scattered into the line of sight by dust particles. At greater distance from the Sun it is called the zodiacal light.
- The **K corona** derives its name for the German word for continuum, and as the name suggests, it has no Fraunhofer lines. The light from the K corona is also highly polarized, a clue that it arises from Thomson scattering of photospheric photons on electrons in the corona. The Fraunhofer lines do not appear because the high temperature of the coronal electrons gives a large Doppler shift to the photons, which smears out the the lines. The high temperature of the corona was suggested to Grotrian in 1931 by this line of reasoning. (A simpler argument for the high temperature is the large hydrostatic scale height implied by the radial density gradient estimated from eclipse observations.)
- Finally, the third component of coronal emission is the **E corona,** produced by the coronal gas itself. The integrated E corona is orders of magnitude fainter than the F and K components, but the emission is concentrated into spectral lines, and in these lines the emission is strong relative to the background of scattered light.

Movie of the wobble of the F-corona (Zodiacal light) throughout the year.

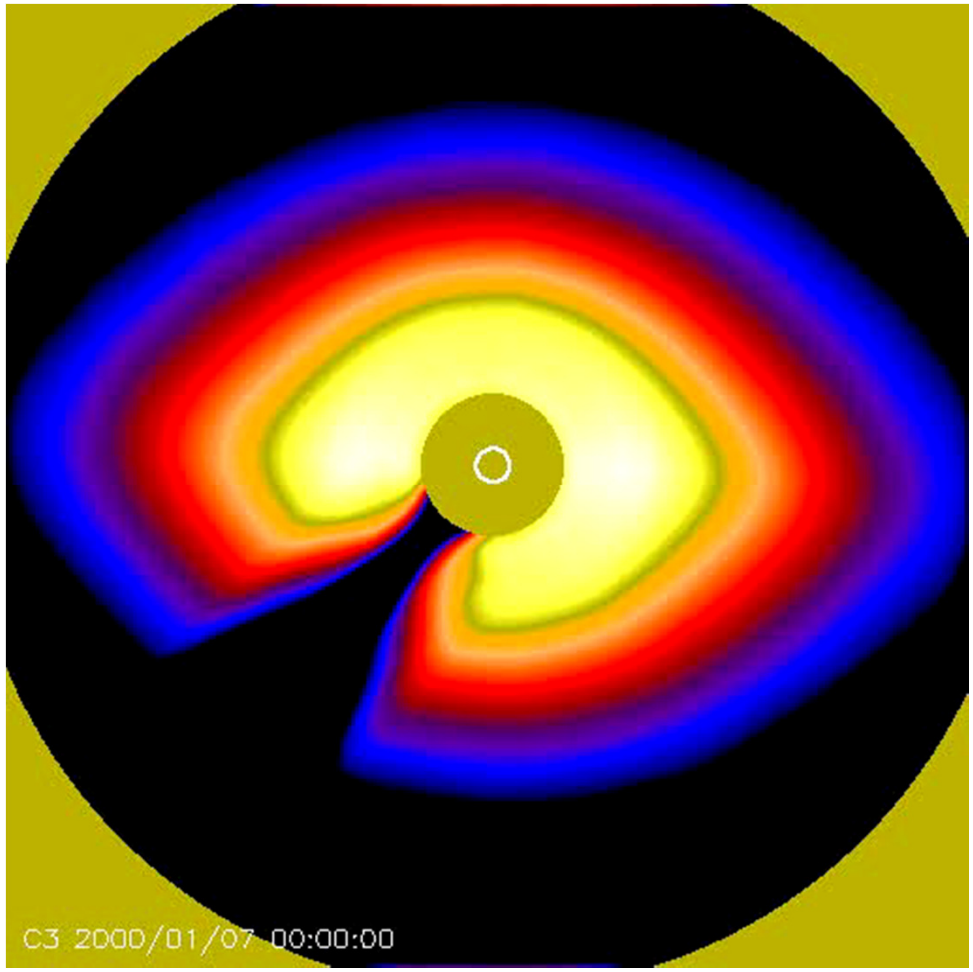

C3 Movie of the wobble of the F-corona (Zodiacal light) throughout the year.
This wobble is due to the difference between the plane of the solar equator and the plane of symmetry of the F-corona. The dust forms a thick pancake-shaped cloud around the Sun. The dust particles are between 10 and 300 micrometres in diameter, most with mass around 150 micrograms.

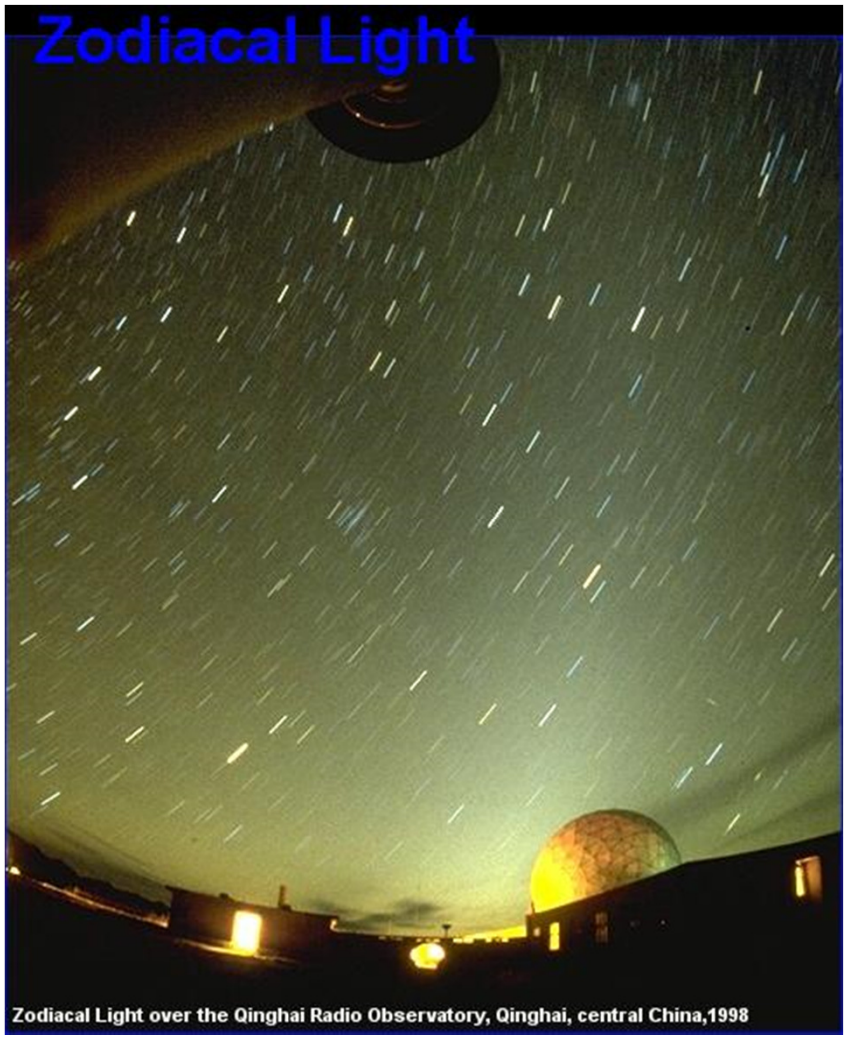

The dust released into our solar system by comets and asteroids undergoes a complex evolution. Initially distributed in the trails that cause meteor showers, the dust eventually disperses into the ecliptic plane (the ecliptic plane is the plane in which the planets move around the Sun). The smallest dust particles are blown out of the solar system by the Sun's radiation. The larger dust particles gradually spiral inwards towards the Sun, and together form a flattened disc in the ecliptic plane in the inner part of the solar system. This disc of dust is composed of dust particles with sizes between 0.1 and 100 micrometer.

From a dark secluded location, this disc of dust is visible from earth at night. A very faint band of light stretches over the sky following the path of the ecliptic ("zodiak").

Zodiacal light over the PMO Qinghai Radio Observatory near Delingha, Northwest Qinghai, central China, 19 November 1998. The observatory lies at 3200 m altitude in the desert. The morning light is visible as the pyramidical light cone at an angle over the observatory dome. Note the small meteor right of the dome.

Dust Origins

Interstellar Dust

Origin in other stellar systems

Permeates interstellar medium; just “passing through.”

Often high velocities, hyperbolic orbits

Interplanetary Dust

Origin from comets and asteroids

Asteroid and short-period comets: dust in ecliptic plane

Long-period comets (source in the Oort Cloud) populate all inclinations and thus are the source of most dust outside the ecliptic plane.

Interplanetary Dust composes up to 70% of dust near the Sun.

Zodiacal light – F-corona

K-corona observed by Mauna Kea coronagraph

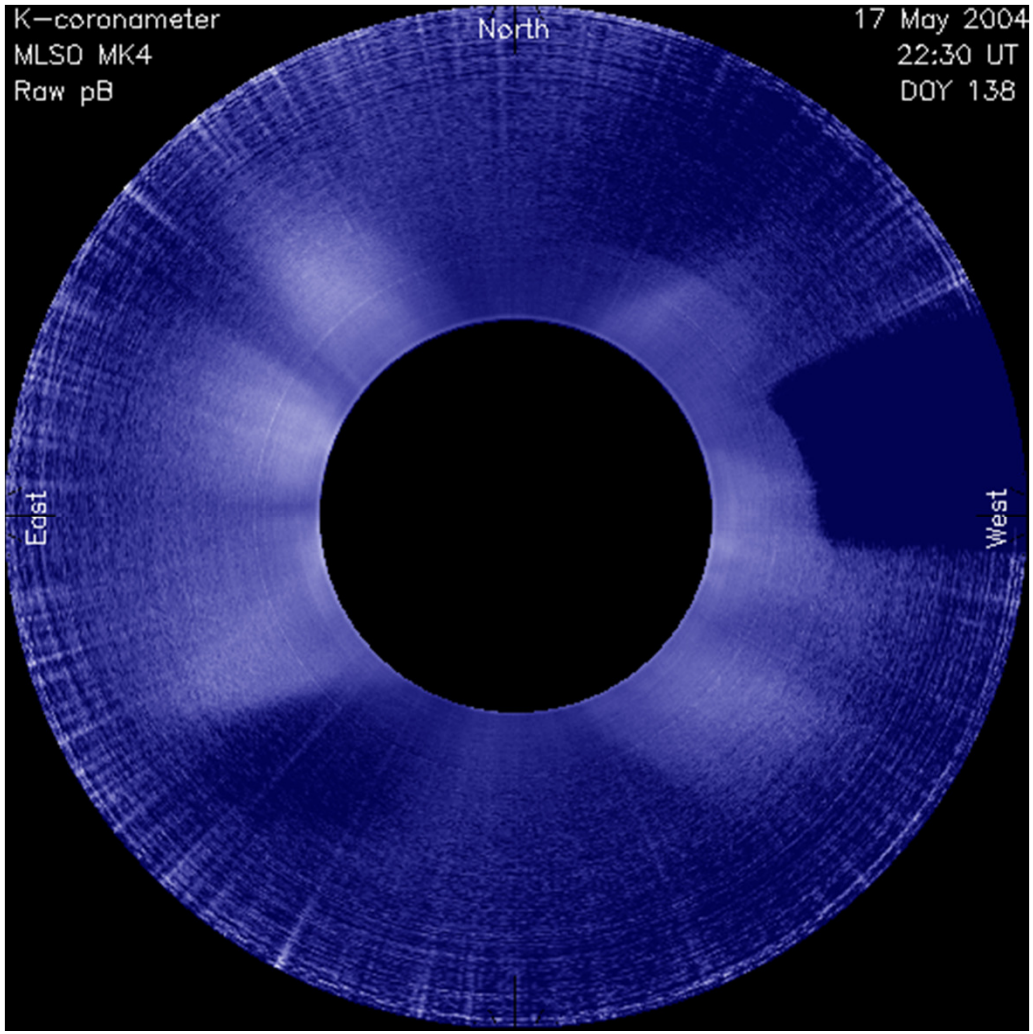

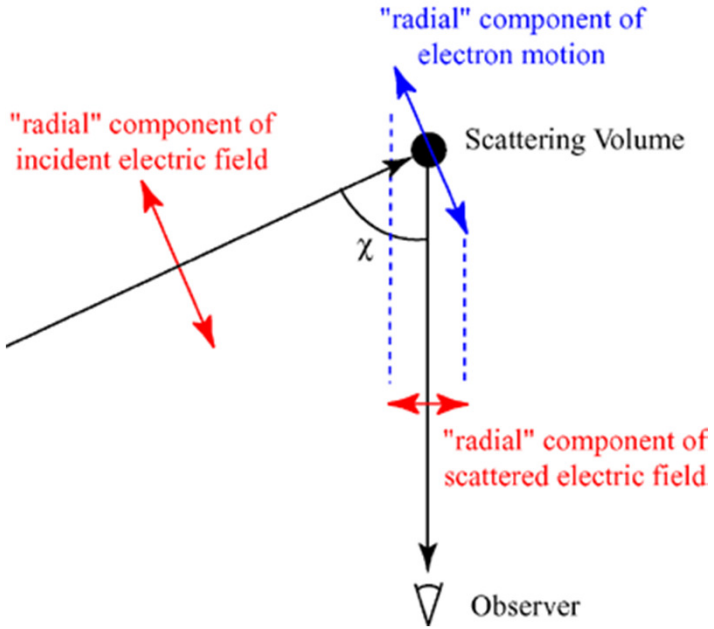

Geometry of Thompson scattering of light on free electron

The light from the K corona arises from Thomson scattering of photospheric photons on electrons in the corona.

Estimate the density of the K corona

Estimate the density of the K corona from the measured intensity $I_K \sim 10^{-6} I_\odot$. The intensity of the scattered light along a characteristic distance of $\sim R_\odot$ is

$$I_K \simeq \sigma_T N_e R_\odot I_\odot,$$

where the cross-section of Thompson scattering is

$$\sigma_T = 3.3 \times 10^{-25} \quad \text{cm}^2.$$

Then,

$$N_e \simeq \frac{I_K}{\sigma_T R_\odot I_\odot} \simeq 4 \times 10^7 \quad \text{cm}^{-3}.$$

Total eclipses are rare (they occur about twice every three years), so they are of limited use in studying the corona. A coronameter is a device which permits the routine observation of the white-light corona by occluding the disk of the Sun and producing images from the polarized light of the K corona.

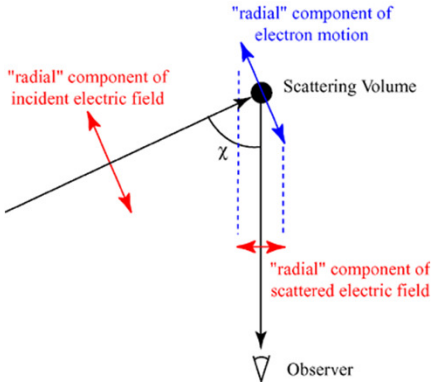

Geometry of Thompson scattering of light on free electron

E-corona: Emission lines

Early observations of the visible spectrum of the corona revealed bright emission lines at wavelengths that did not correspond to any known materials. This led astronomers to propose the existence of "coronium" as the principal gas in the corona. The "red" line at 6375Å was indentified a forbidden transition ${}^2P_{1/2} \rightarrow {}^2P_{3/2}$ in Fe X.

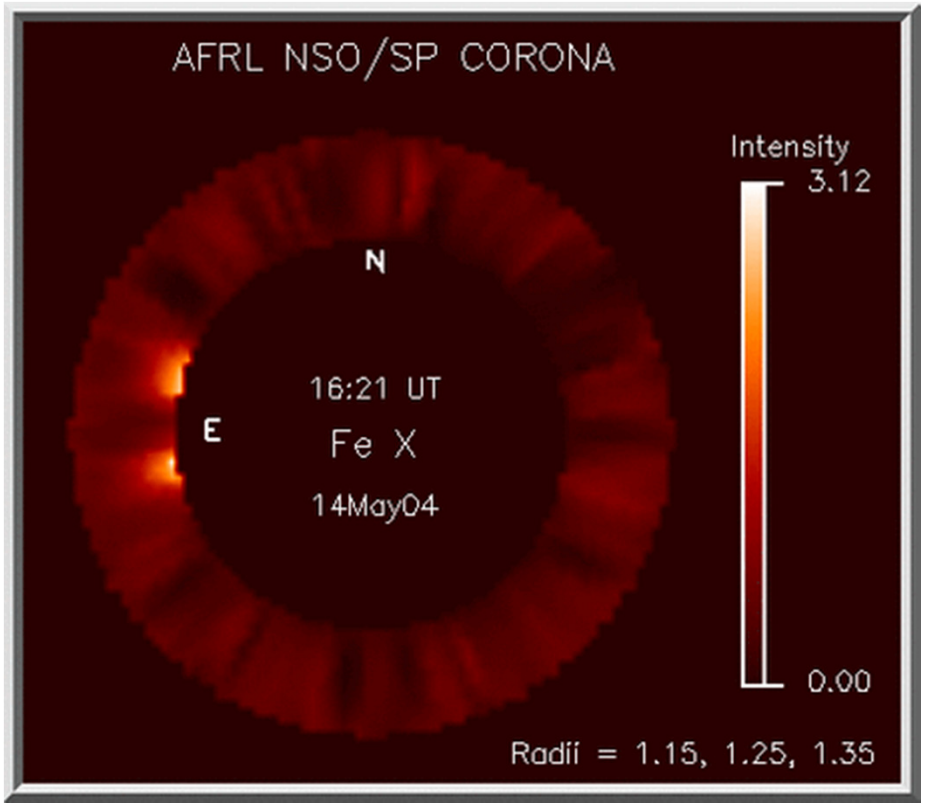

A Fe X image of the corona of March 5, 2002,from the National Solar Observatory

A Fe XIV 5303A "Green line" image of the corona of March 5, 2002, from the National Solar Observatory.

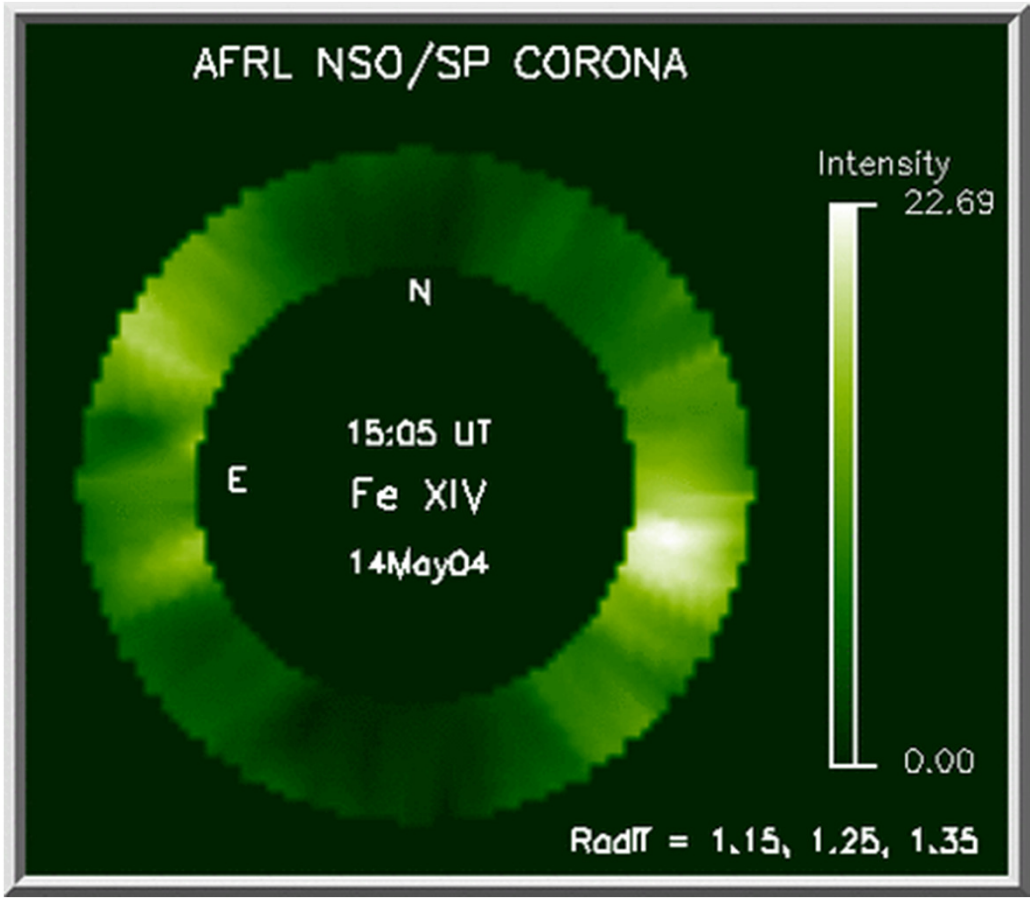

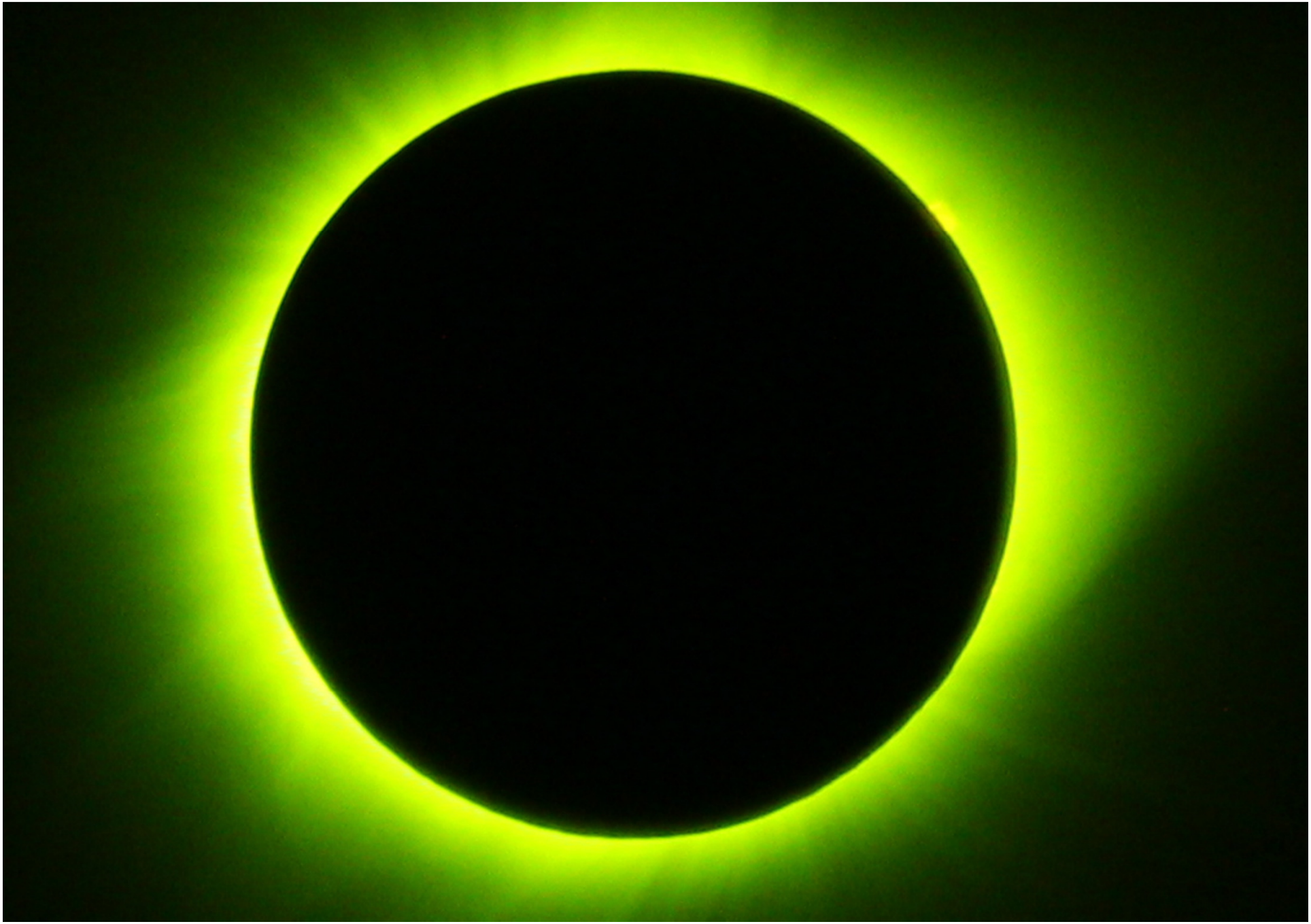

High-resolution image of E-corona in Fe XIV line

Image of the corona from SDO/AIA in Fe XII 193A line

(Fe XII - 11 times ionized iron)

Coronal hole

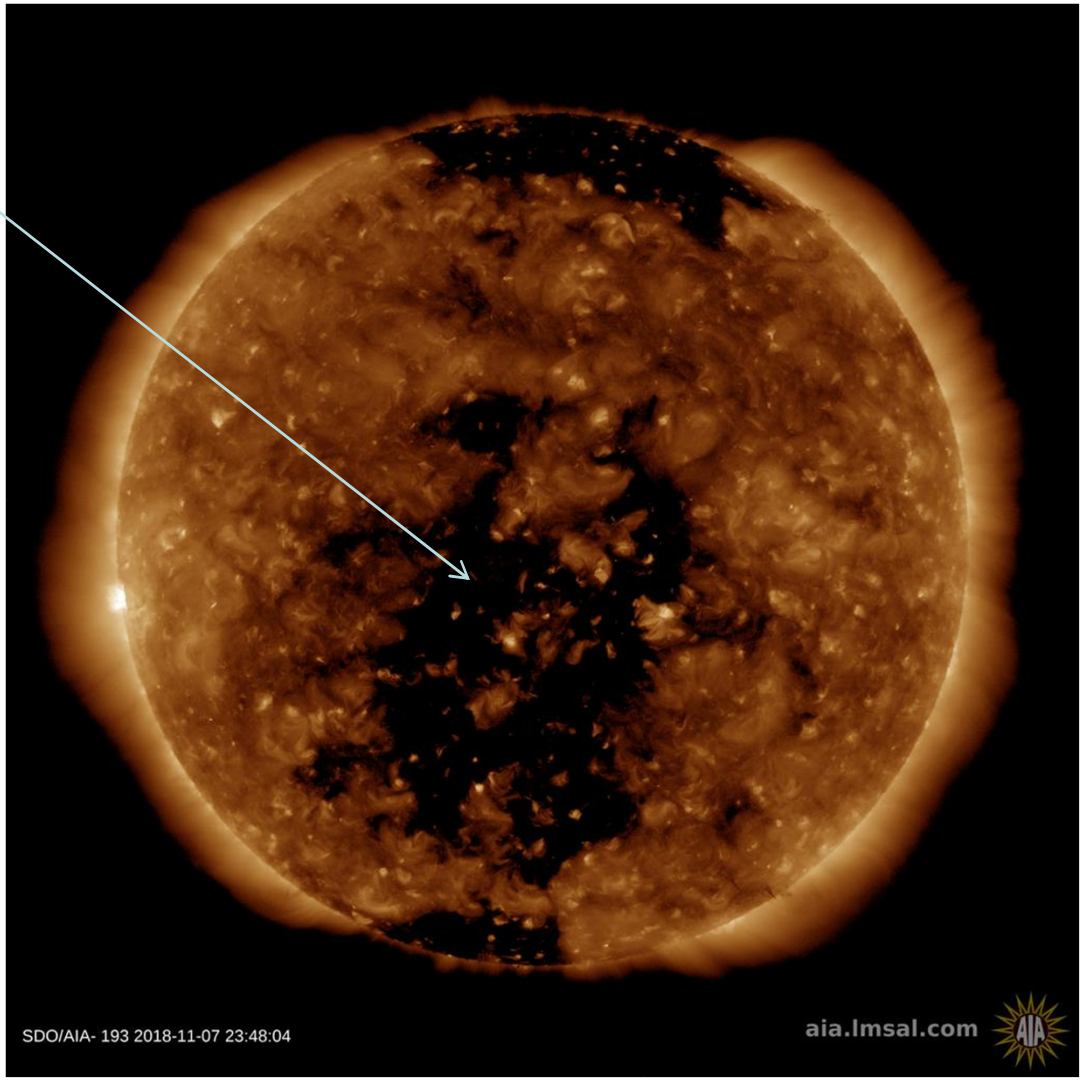

The E-corona is best observed in the extreme ultraviolet and in X-ray, but because the atmosphere blocks these short wavelengths, the observations must be made from space.

X-Ray Emission

Soft X-ray and UV emission from the corona consists of free-free emission ('bremsstrahlung') and bound-free emission, which produces a continuum, and also line emission from partially ionized elements.

Skylab in 1973 provided the first detailed study of the solar corona in soft (low-energy) X-rays. It revealed that the soft X-ray emitting plasma of the corona is everywhere structured into loops, except in dark coronal holes that occur predominantly at the poles.

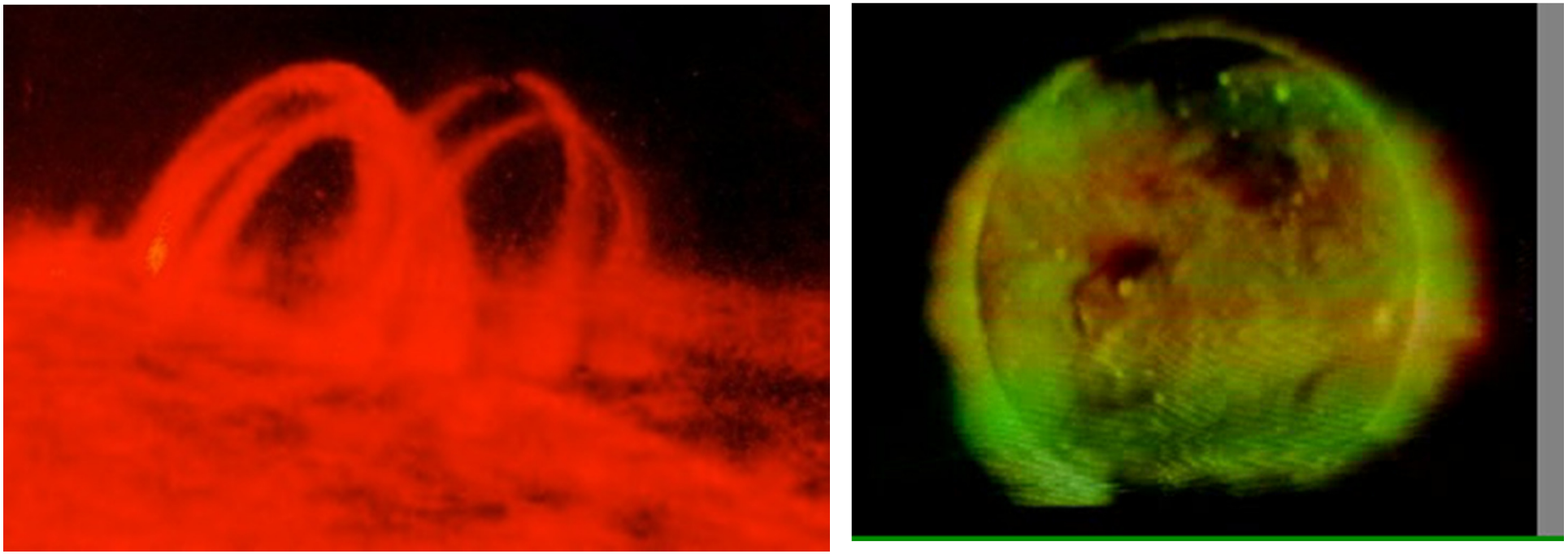

The Sun observed by Skylab in X-rays with wavelengths from 6 to 49 Å.

Recent soft X-ray image of the solar corona from XRT on Hinode

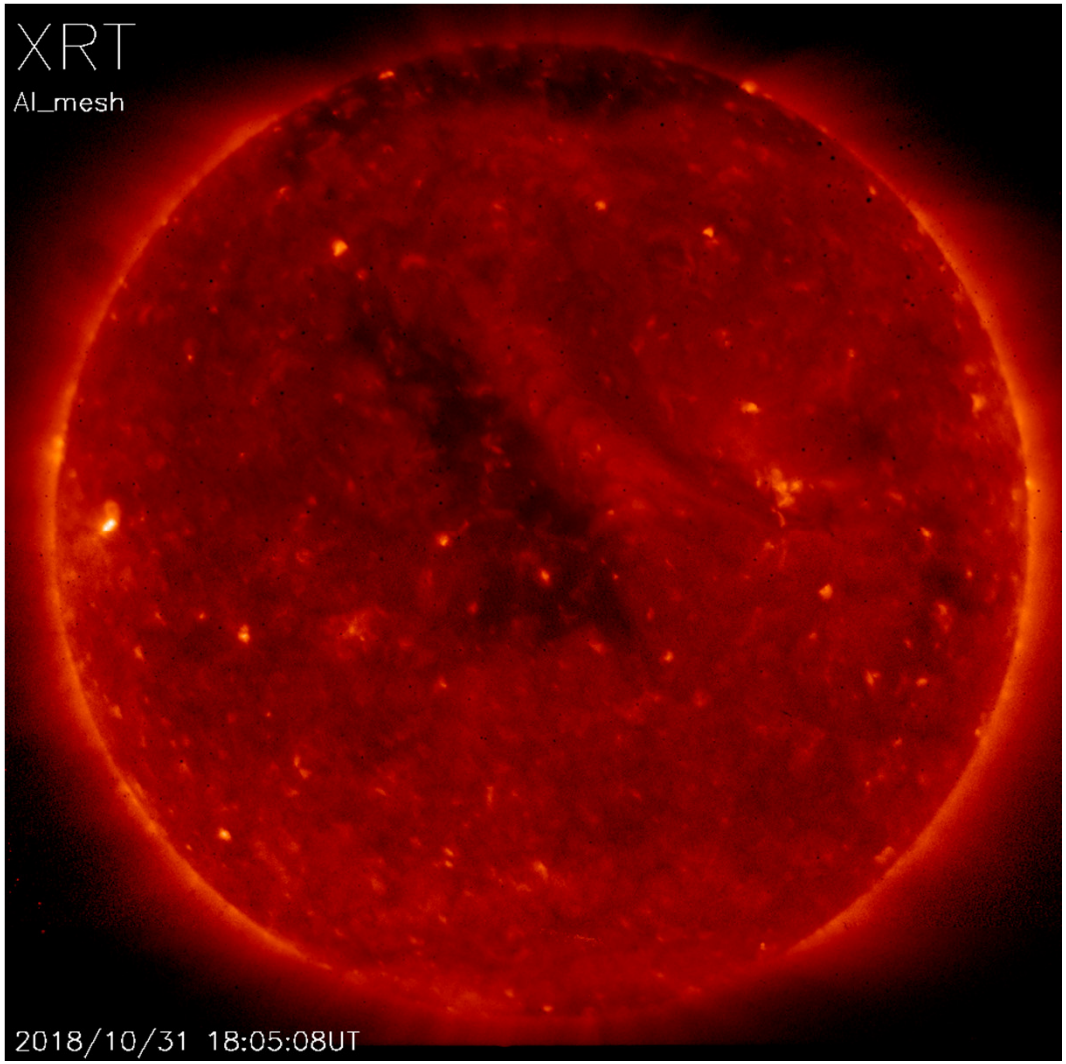

X-Ray Telescope (XRT) on Hinode satellite provides 2-arcsecond resolution images of the highest temperature solar coronal material, from 1,000,000 to 10,000,000 Kelvin (the energy range 0.2 to 1.2 keV)

Coronal structures

Soft X-ray **coronal loops** are believed to delineate the magnetic field, and represent closed field regions, i.e. regions where the magnetic field leaves and then returns to the Sun.

Coronal holes are open field regions, where the magnetic field has a predominant polarity, and leaves the Sun (it must eventually return, but the closure of open field lines occurs at large distances from the Sun).

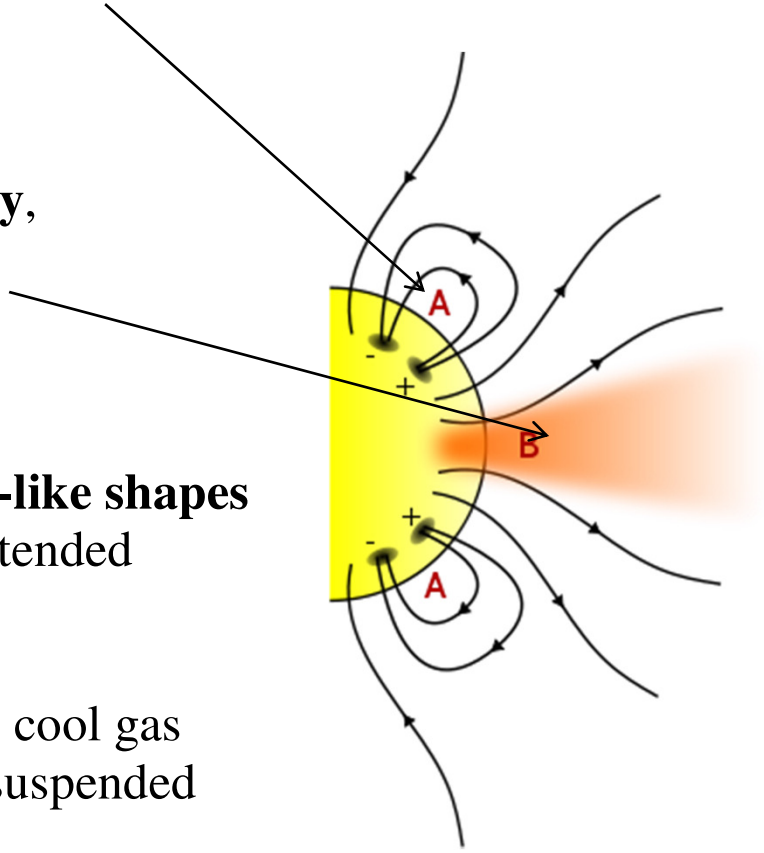

Extended magnetic configurations with cusp-like shapes are helmet streamers, that underlay similar extended structures seen in white light.

Prominences are long-lived intrusions of dense, cool gas that arise due to a radiative instability, and are suspended in the hot corona by magnetic forces.

The reason for the dominance of the magnetic field in the corona is that the ratio of gas pressure to magnetic pressure is very small. The brightest loops occur around active regions, pointing to the central role of the magnetic field in coronal heating. The corona in X-ray also reveals other structures.

Emission of the solar corona

The emission in a spectral line of a m -times ionized element X^{+m} occurred by transition from a level j to level i :

$$X_j^{+m} \rightarrow X_i^{+m} + h\nu_{ij}.$$

This is bound-bound emission. The emissivity is given by:

$$P_\nu = N_j(X^{+m}) A_{ji} h\nu_{ij} \psi_\nu,$$

where $N_j(X^{+m})$ is the number density of X^{+m} atom in level j, A_{ji} in the Einstein spontaneous emission coefficient, ψ_ν is the normalized emission profile ($\int \psi_\nu d\nu = 1$).

Coronal approximation: level j is populated from the level i by collisions with thermal electrons. Level j depopulated only by the radiative decay to lower levels.
Then, the emissivity can be reduced to the relation:

$$P_{ij} = A_X G(T, \lambda_{ij}) \frac{hc}{\lambda_{ij}} N_e^2,$$

where A_X is the abundance of element X relative to hydrogen, λ_{ij} is the wavelength, $G(T, \lambda_{ij})$ is called the contribution function, N_e is the electron density.

Differential Emission Measure

The flux $I(\lambda_{ij})$ at distance R:

$$I(\lambda_{ij}) = \frac{1}{4\pi R^2}\int_V P_{ij}\,dV = \frac{1}{4\pi R^2}\int_V A_X G(T,\lambda_{ij})\frac{hc}{\lambda_{ij}} N_e^2\,dV$$

or

$$I(\lambda_{ij}) = \frac{1}{4\pi R^2} A_X \int G(T,\lambda_{ij})\frac{hc}{\lambda_{ij}} Q(T)\,dT,$$

where $Q(T)$ is **the differential emission measure (DEM)** defined as

$$N_e^2\,dV = Q(T)\,dT.$$

The DEM is a measure of the amount of emitting material as a function of temperature in the coronal plasma.

The emitted power by a solar region:

$$L = 4\pi R^2 I = \int N_e^2 \mathscr{P}(T)\,dV = \int Q(T)\mathscr{P}(T)\,dT, \quad \text{erg / s},$$

where $\mathscr{P}(T)$ is the plasma radiative loss function.

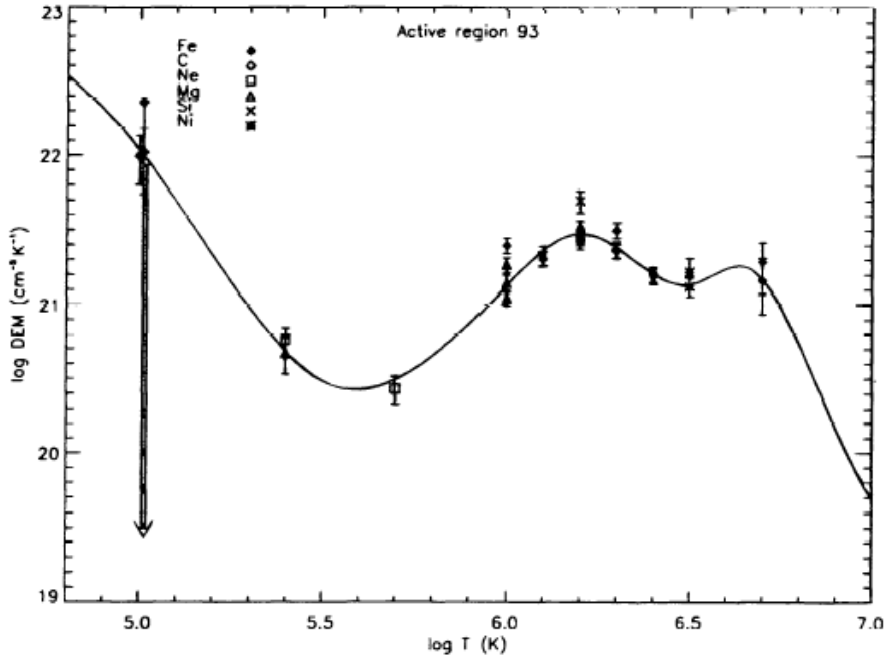

FIG. 8*a*

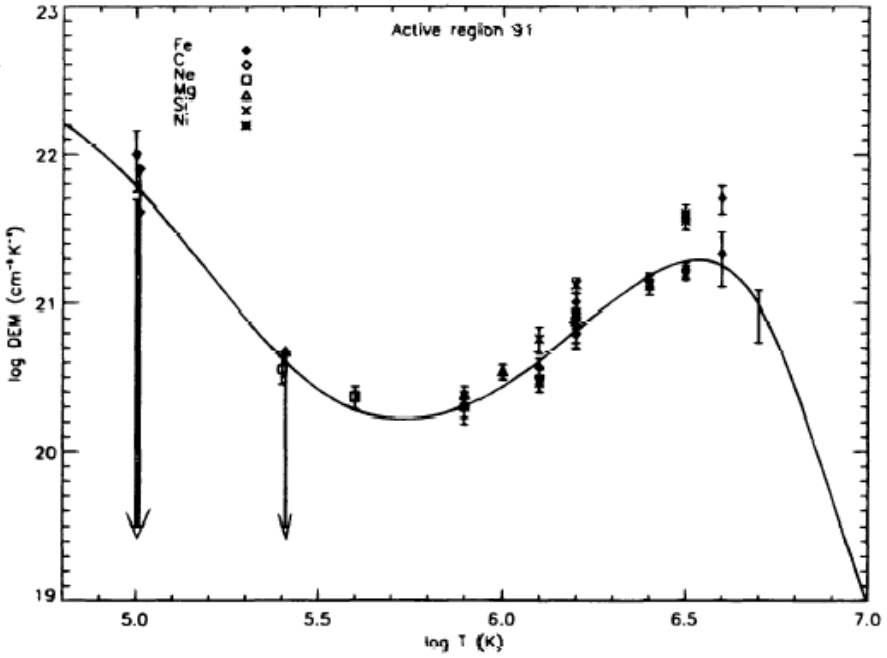

Examples of the Differential Emission Measure for an active region and for a quiet corona.

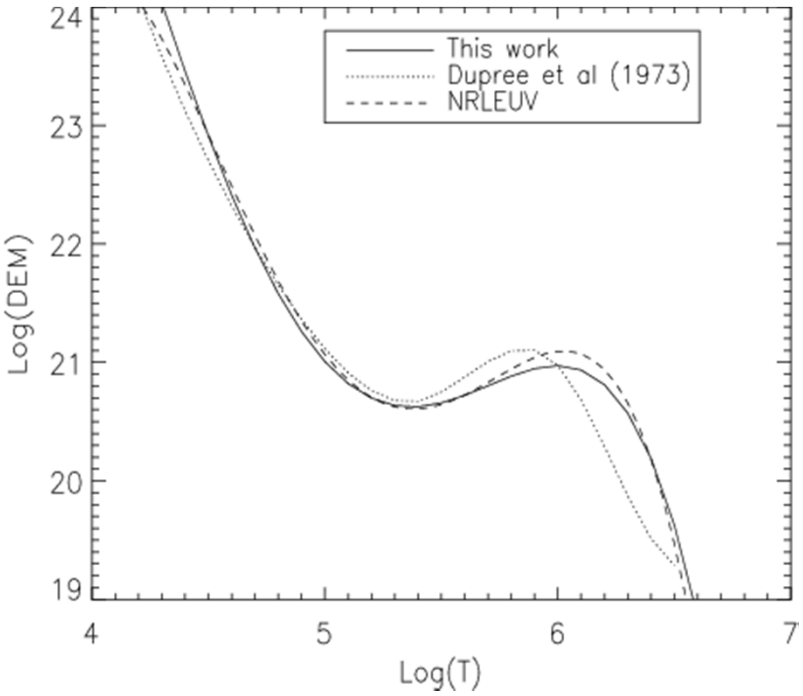

DEM of the quiet Sun from SOHO/SUMER data (Kretzschmar, 2004)

The radiative loss function $\mathscr{P}(T)$ and its contributors.

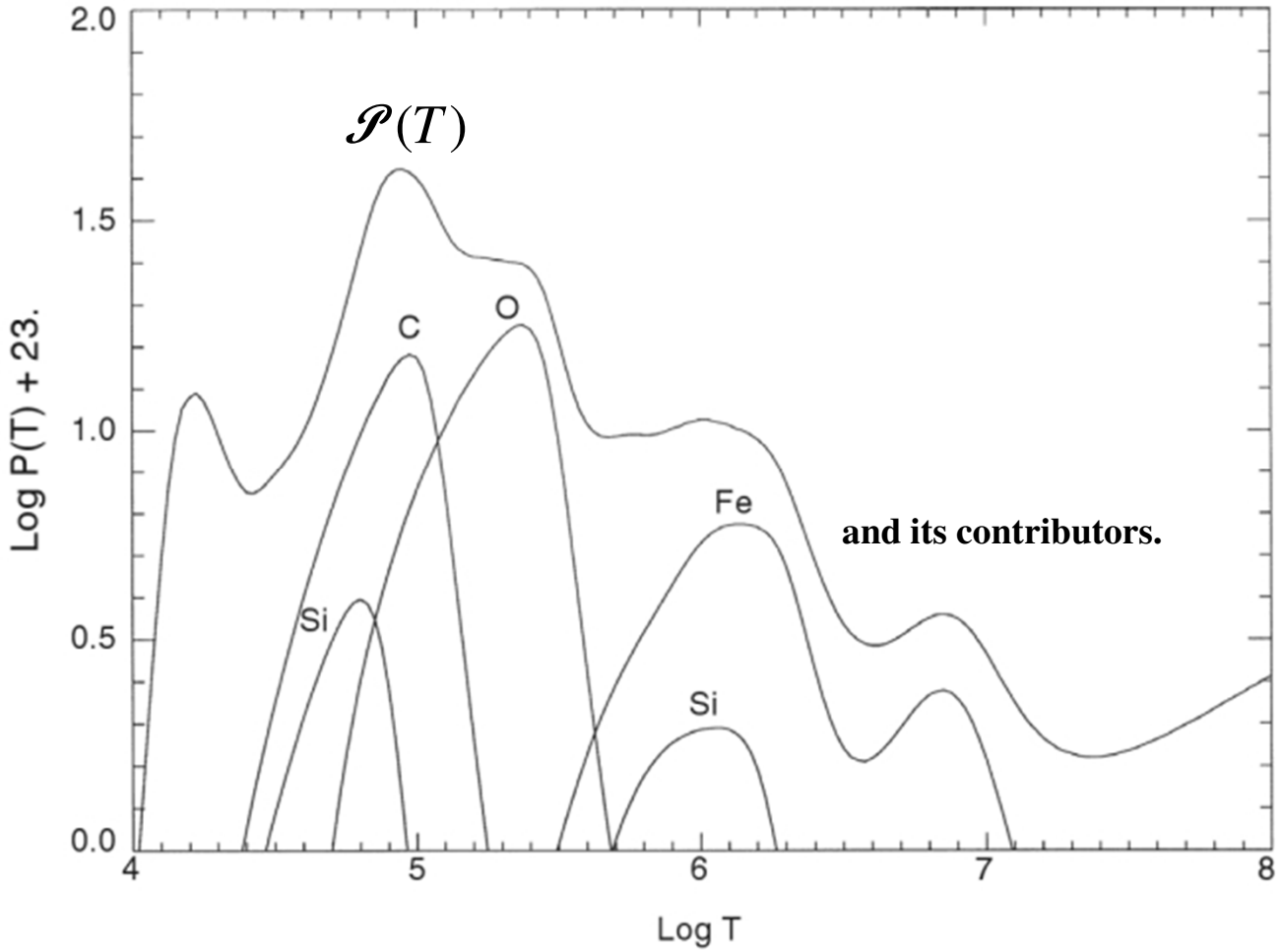

The radiative losses in the corona (logT>6) decrease with increase of temperature making possible the development of thermal instabilities.

For optically thin plasma the radiative loss rate is given by $E_R = N_e N_p \mathscr{P}(T)$.

The radiative loss function can be approximated as $\mathscr{P}(T) = P_0 T^{-1/2}$.

Scaling Laws for Coronal Loops

X-ray images of the corona show that it consists of bright loop structures and dark areas ("coronal holes") which correspond to areas of open magnetic field.
Consider the thermal structure of a static loop. The energy balance along the loop may be written

$$E_h(s) = Q(T) - \frac{d}{ds}\left[\kappa \frac{dT}{ds}\right],$$

where s is the coordinate along the loop, κ is the thermal conductivity

$$\kappa = \kappa_0 T^{5/2},$$

E_h is the energy input, and $Q(T) = N_e^2 \mathcal{P}(T)$ is the radiative energy losses.

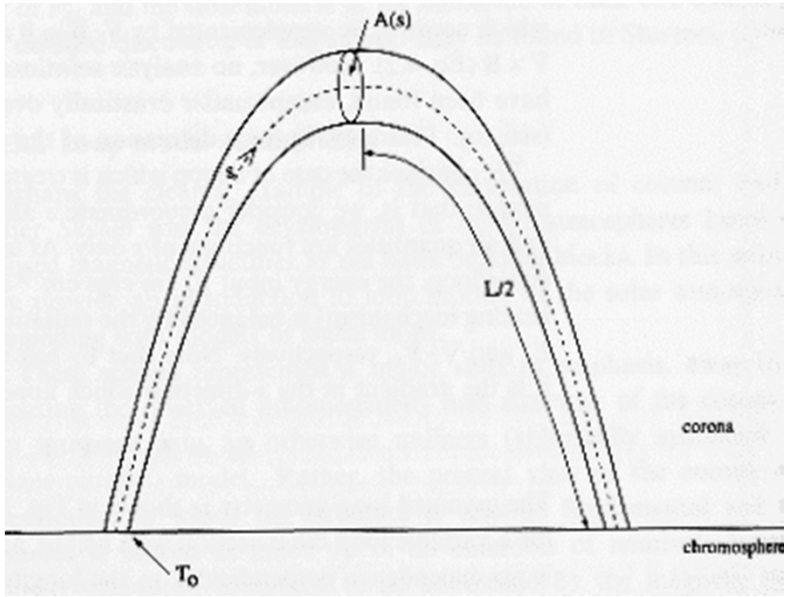

Equation for temperature distribution along the loop

Consider the energy equation: $E_h(s) = Q(T) - \frac{d}{ds}\left[\kappa \frac{dT}{ds}\right]$.

If the energy input is a function of temperature: $E_h = H_0 T^{\beta}$

and the energy loss rate is: $Q(T) = N_e^2 \mathcal{P}(T) = K_0 \frac{P^2}{T^2} \mathcal{P}(T)$ where $\mathcal{P}(T) \propto T^{-1/2}$

then: $H_0 T^{\beta} = K_0 \frac{P^2}{T^2} T^{-1/2} - \frac{d}{ds}\left(\kappa_0 T^{5/2} \frac{dT}{ds}\right)$,

where P is the pressure, and we used the equation of state ($P = R\rho T \propto N_e T$); K_0 is a constant.

Then $$\frac{d}{ds}\left(\kappa_0 T^{5/2} \frac{dT}{ds}\right) = K_0 P^2 T^{-5/2} - H_0 T^{\beta}$$

or $$\frac{7}{2}\kappa_0 \frac{d^2 T^{7/2}}{ds^2} = K_0 P^2 T^{-5/2} - H_0 T^{\beta}.$$

This equation specifies the temperature distribution along the loop.

Rosner-Tucker-Vaiana relation

Consider the case of a constant heating function (β=0), and look for an approximate solution in the form

$$T \sim T_m (s/L)^{\alpha},$$

where T_m is the maximum temperature at the loop top, L is the half-length.

Then for α we obtain the relation:

$$\frac{7}{2}\alpha - 2 = -\frac{5}{2}\alpha.$$

That is $\alpha = 1/3$.

Then for the parameters T_m and L we get a simple estimate:

$$\left(\frac{T_m}{L^{1/3}}\right)^{7/2} = K_0 P^2 \left(\frac{T_m}{L^{1/3}}\right)^{-5/2}.$$

Finally,

$$T_m = K_0^{1/6} (PL)^{1/3}.$$

This is the **Rosner-Tucker-Vaiana relation** between the maximum temperature, pressure and the length of the loop. It was found that this relation fits the observations quite well.

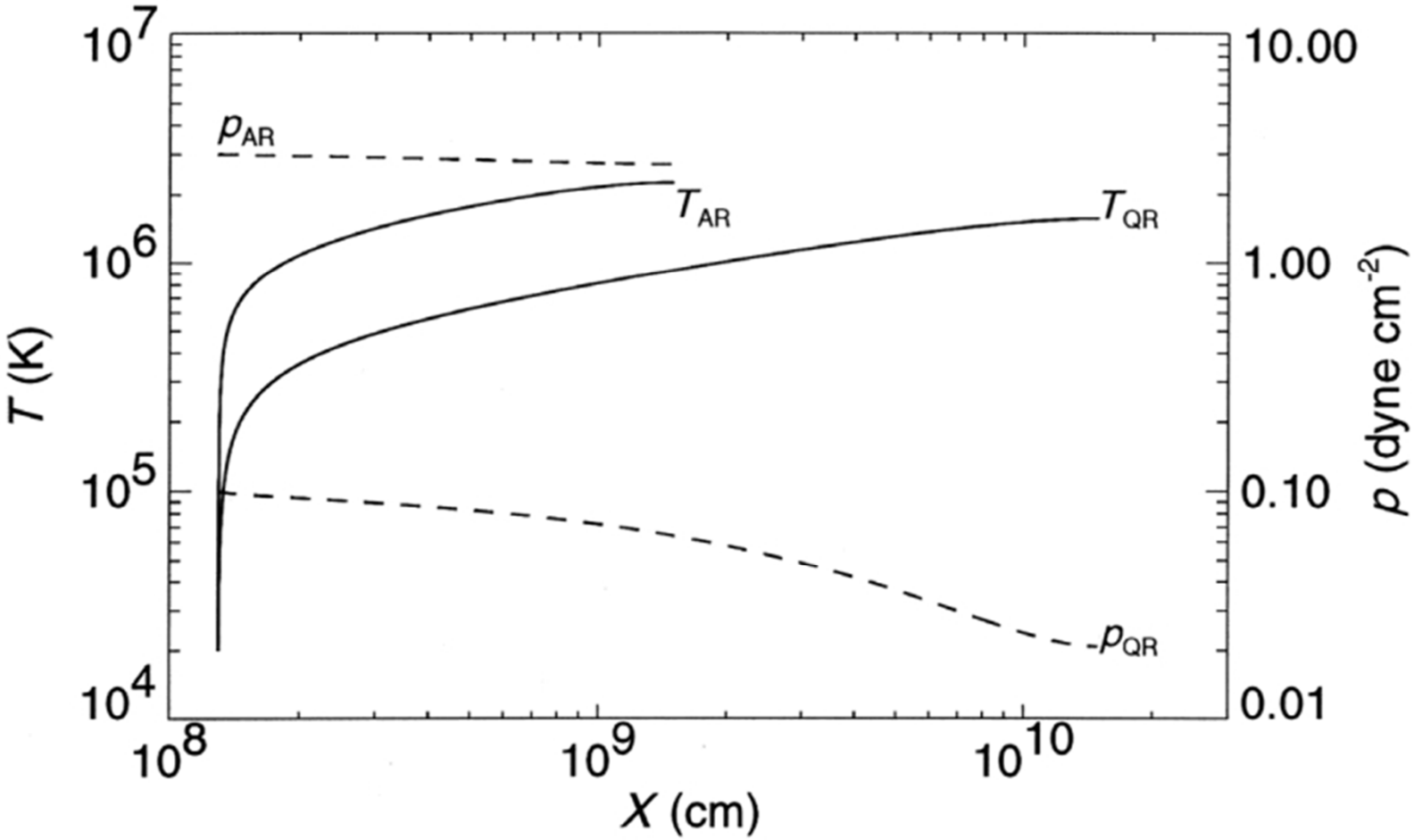

Numerical solution to the static loop model for a compact active region loop (AR) with $L = 15{,}000$ km, $P = 3$ erg cm^{-3}, and a quiet region loop (QR) with $L = 150{,}000$ km, $P = 0.1$ erg cm^{-3}.

Coronal Heating Models (from Mandrini et al. 2000)

Physical process	References
DC ("Direct Current") Stressing and Reconnection Models:	
– Stress-induced reconnection	Sturrock & Uchida (1981) Parker (1983, 1988)
– Stress-induced current cascade	Van Ballegooijen (1986)
– Stress-induced turbulence	Heyvaerts & Priest (1992)
. AC (Alternating Current) Wave Heating Models:	
– Alfvénic resonance	Hollweg (1985, 1991)
– Resonant absorption	Ionson (1978, 1982, 1983), Mok (1987))
– Phase mixing	Heyvaerts & Priest (1983)
– Current layers	Galsgaard & Nordlund (1996)
– MHD Turbulence	Inverarity & Priest (1995b)
– Cyclotron resonance	Hollweg (1986), Hollweg & Johnson (1988)
. Acoustic Heating:	Schatzman (1949)
– Acoustic waves	Kuperus, Ionson, & Spicer (1981)
. Chromospheric Reconnection:	Litvinenko (1999)
. Velocity Filtration:	Scudder (1992a,b; 1994)

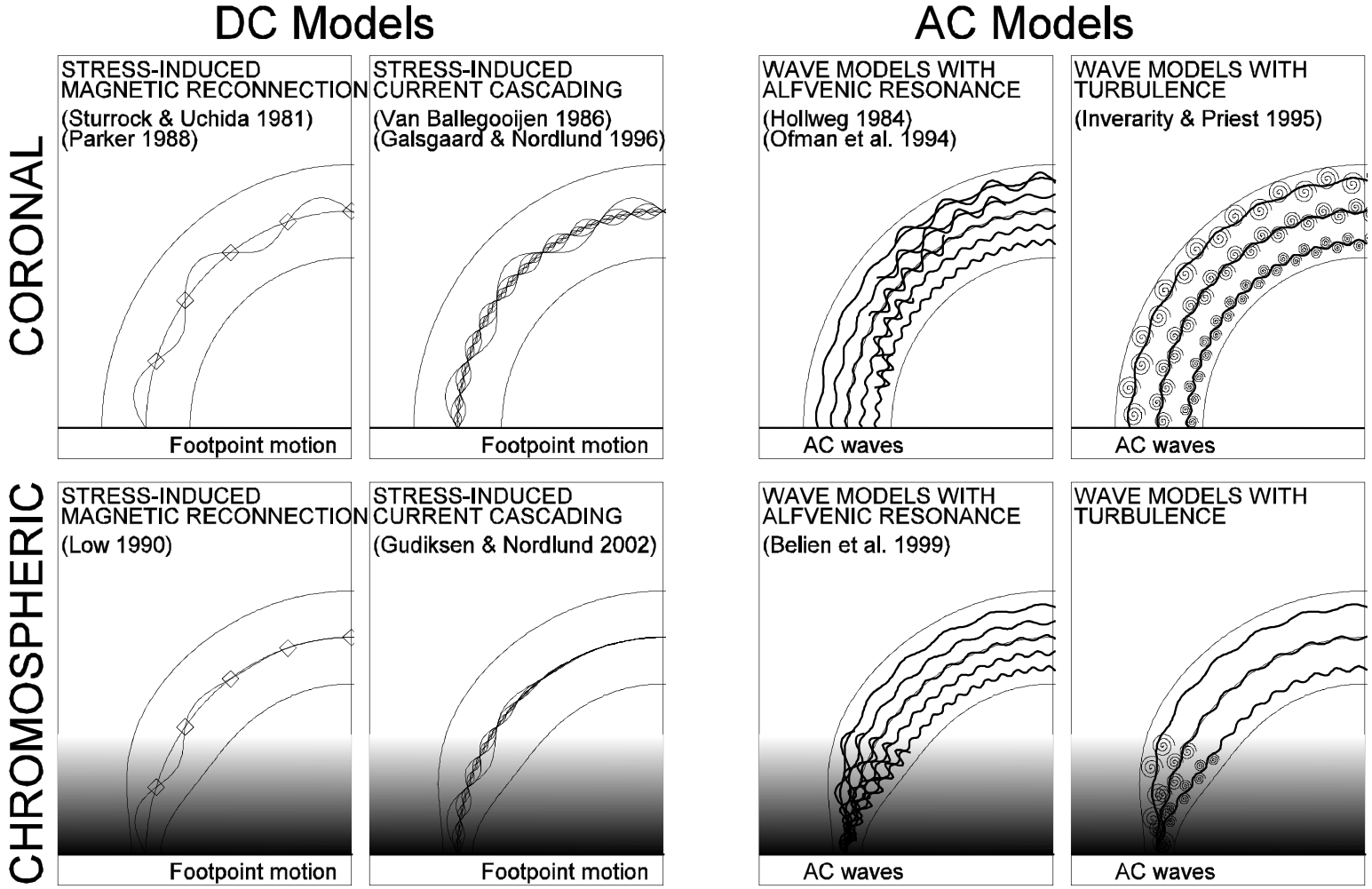

Categories of DC (left panels) and AC models (right panels), subdivided into coronal (top row) and chromospheric versions (bottom row). The greytones demarcate high-density regions (chromosphere and transition region) (Aschwanden 2002b).

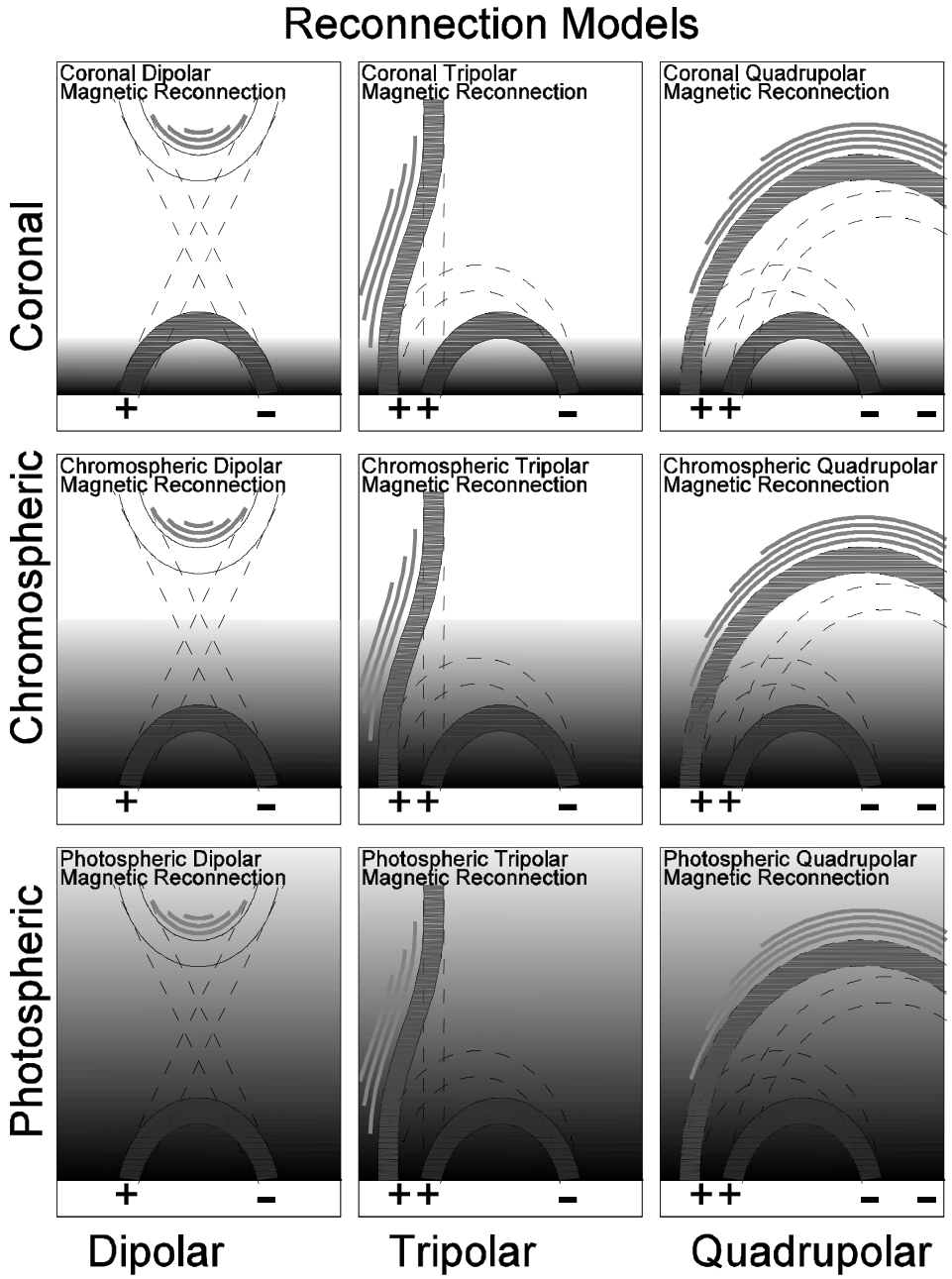

Basic categories of magnetic reconnection models, subdivided into coronal (top row), chromospheric (middle row), and photospheric versions (bottom), and according to bipolar (left column), tripolar (middle column), and quadrupolar (right column) configurations. The magnetic polarities are indicated with + and – signs. The greytones show high-density regions (photosphere, chromosphere, transition region). The dashed lines symbolize the pre-reconnection configuration, and the solid lines show the post-reconnection configuration, rendered in grey if the new-configured field lines have been filled with heated high-density plasma. The grey curves indicate shock waves or high-frequency acoustic waves (Aschwanden 2002b).

DC Heating models: stress-induced reconnection

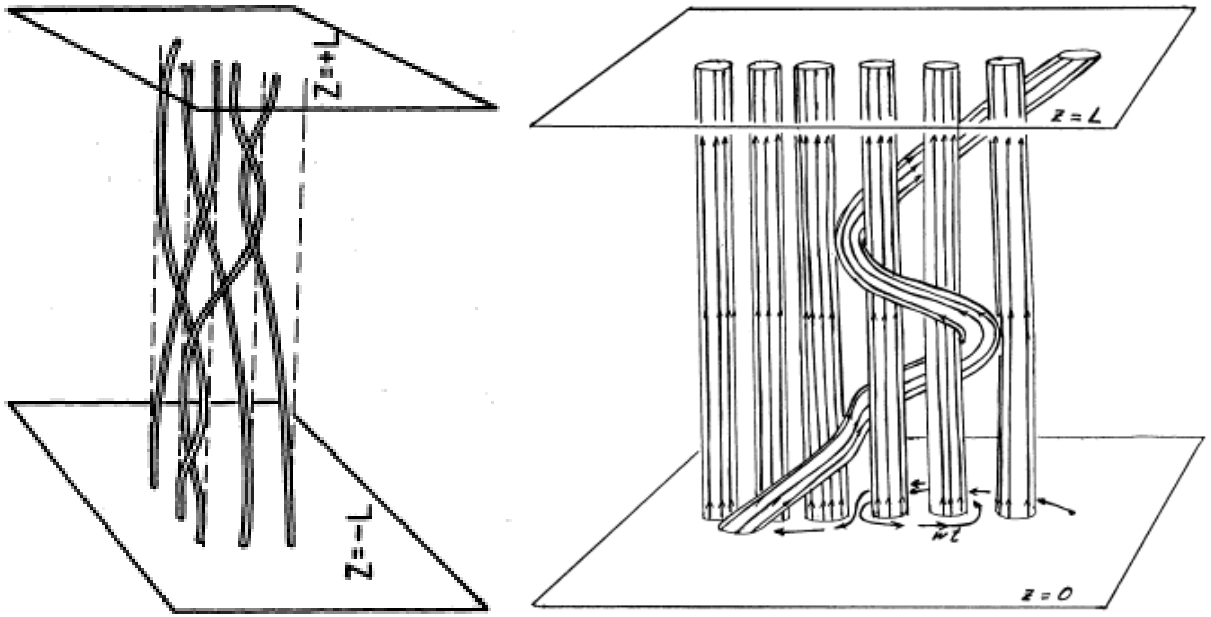

Cartoons of the topology of magnetic flux tubes that are twisted by random walk footpoint motion (left; Parker 1972), leading to a state where fluxtubes are wound among its neighbors (right; Parker 1983).

New ideas: coronal heating by nanoflares (Brosius et al, 2014)

The sounding rocket carrying the EUNIS experiment: Extreme Ultraviolet Normal Incidence Spectrograph.

The EUNIS spectrograph was tuned into a range of wavelengths useful for spotting material at temperatures of 10 million Kelvin – temperatures that are a signature of nanoflares.